Cooling of large molecules below 1 K and He clusters formation

U. Even,[a] J. Jortner, D. Noy, and N. Lavie
Sackler Faculty of Exact Sciences, School of Chemistry, Tel Aviv University, Ramat Aviv, 69978 Tel Aviv, Israel

C. Cossart-Magos
Laboratoire de Photophysique Moléculaire CNRS, Université de Paris-Sud, Bâtiment 210, 91405 Orsay Cedex, France

(Received 25 October 1999; accepted 8 February 2000)

We present here the design details of a high-pressure pulsed valve that generates intense supersonic jets. The measured rotational contours of Aniline indicate that temperatures lower than 0.5 K can be achieved before the formation of clusters with the He carrier gas. The spectral shifts and vibronic structure of Anthracene–He_n clusters ($n=1-6$) are showing some surprising features. © *2000 American Institute of Physics.* [S0021-9606(00)01117-X]

I. INTRODUCTION

Supersonic jets have been used successfully to generate jets of cold and isolated molecules since the pioneering work of Levy, Wharton, and Smalley more than two decades ago.[1] Continuous nozzles,[2,3] as well as pulsed valves at ambient or elevated temperatures,[4] are routinely used to generate supersonic jets and cool large molecules to remove vibrational spectral congestion with rotation temperature down to ~2 K. The list is too long to do justice to all. The cooling achieved by the expanding carrier gas is well understood, modeled, and documented. The (heavy) molecule is first accelerated to the (light) carrier gas velocity (~1750 m/s for room temperature He) and the internal modes energy (vibrations and rotation) is then carried away by a soft (small relative velocity) collision in the jet. The achieved cooling is determined by the total number of collisions experienced by the molecule until the carrier gas is so rarefied downstream that the cooling is terminated. The cooling is thus a result of two body collisions in the jet. When the molecule is cold enough it can adsorb carrier gas atoms and form clusters. Clustering requires additional cooling to remove the condensation energy, and proceeds in a stepwise fashion. Quantum dynamics require three body collisions to generate a bound cluster. Thus, it is not surprising that cooling down to 2–4 K can be achieved (a temperature that is lower than the bulk condensation temperature of the carrier gas) prior to clustering.[5] The question we ask is how low can we push the limit of cooling before clustering occurs. The answer is that we can get down to ~0.5 K for the bare molecule. Small He clusters will then grow on the molecule and further cooling is stopped.

The ability to cool molecules below 1 K facilitates the exploration of ultracold molecular physics and collisions.[6] Photoassociation of laser cooled alkali atoms produced Cs_2 molecules with translation temperatures of 300 μK.[7] A successful approach toward the same goal was undertaken by using a cryogenic (20 K), continuous-flow, nozzle to form giant clusters of He (containing 10^3-10^6 atoms). These clusters then pick up the vaporized molecules and subsequently cool the molecule by He evaporation.[8] Both atoms and large molecules in He clusters were probed.[9,10] A temperature of ~0.4 K was reported.[8] Recently, magnetic trapping and cooling in ^{3}He was reported for paramagnetic diatomic molecules.[11] The achieved temperature was similar to that obtained by us (0.4 K). In this paper we report on the cooling of large molecules in pulsed, high-pressure, supersonic expansion of room temperature He down to 0.4 K.

We describe the construction and operating properties of a new high-pressure pulsed valve nozzle. Rotational cooling of Aniline at 0.4 ± 0.1 K was achieved. We also describe cold cluster production and analyze the spectra of Anthracene–He_n clusters ($n=1-6$).

II. A HIGH-PRESSURE VALVE

It was clear to us from the beginning that high-pressure operation will benefit from miniaturization of the pulsed valve parts. Two important goals can be achieved by miniaturization.

(1) Reduction of the magnitude of the forces due to the high pressure operating on the valve seals.
(2) Reduction of the moving mass (shortening the opening time and cutting the gas throughput).

Extensive computer simulations preceded the construction of the valve. We used a numerical finite element program[12] to solve Maxwell equations for the magnetic field generated by a current carrying coil. The program included magnetic saturation of the magnetic parts and computed the forces and resulting acceleration of the moving parts as well as the heat developed by eddy currents. Trial and error resulted in a simplified and optimized design. The design predicted the actual valve operating properties to within 10%. A schematic cross section drawing of the adopted design is shown in Fig. 1.

[a]Correspondence to be addressed to Professor Uzi Even, Sackler Faculty of Exact Sciences, School of Chemistry, Tel Aviv University, 69978 Tel Aviv, Israel. Electronic mail: even@chemsgl.tau.ac.il; fax: +972-3-6409293

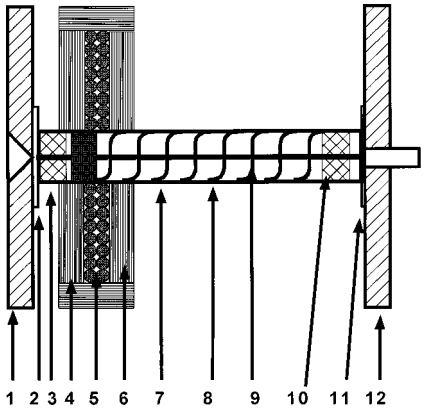

FIG. 1. Fast pulsed valve construction details. (1) Conical nozzle (hole diameter 0.2 mm); (2) front ''Kapton'' foil seal (0.1 mm thick); (3) front ''Vespel'' guide; (4) Front ''Permendur'' magnetic lamination; (5) Kapton insulated copper wire coil; (6) back ''Permendur'' magnetic lamination; (7) ''Hastalloy'' high-pressure tube (2 mm diam 0.2 mm thick); (8) return stainless steel spring; (9) ''high speed'' steel moving hammer; (10) back ''Vespel'' guide; (11) back ''Kapton'' foil seal; and (12) back stainless flange and gas feed.

A high-current pulse (500 A) is generated by discharging an electrolytic 600 μF capacitor. The capacitor is charged to 100 V by a current limiting supply and is discharged through an electronic switch (Insulated Gate Bipolar Transitor[13]) for 20 μs. The high current generates (at the coil center) a magnetic field of 2.5 T, pulling the moving hammer with $\sim$10 N force. The resulting acceleration allows the hammer to complete its free travel of 0.1 mm in 8 μs, and be returned to its sealing position by the spring. The valve operated reliably at up to 25 Hz. It was tested in the temperature range between 120–460 K. The short opening time of the valve generated very little gas load in the first chamber. At 100 bar operating pressure, and at 10 Hz repetition rate, the gas throughput is only 0.01 L Torr/s (nozzle diameter was 0.2 mm). The low throughput required only a small 200 L/s turbo pump to maintain a background pressure of 6×10^{-5} Torr in the first chamber. The short gas pulse generates a packet of fast moving seeded He that is only 15 mm long, which is fully utilized in the mass spectrometer. The gas pulse width was monitored by electron impact ionization near the nozzle exit. The intensity of the He mass peak, as a function of the delay of the ionizing pulse, is shown in Fig. 2. The measured pulse width is $\sim$8 μs. The new valve is, therefore, a highly efficient supersonic jet source and consumes only a few milligrams of material for a complete spectral identification (less than 1 mg/Hr of the investigated molecule). The short packet requires careful laser timing ($\sim$1 μs) to detect it in the mass spectrometer volume. The required time delay (from valve opening to laser firing) allowed us to measure the gas packet velocity directly (1780$\pm$20 m/s for He at 310 K).

III. COOLING IN A HIGH-PRESSURE JET

Using the limited spectral resolution (0.2 cm^{-1} after frequency doubling) of our Yag pumped dye lasers (Continuum ND 6000) we could only interrogate the rotational envelope of Aniline (individual rotation lines could not be resolved).

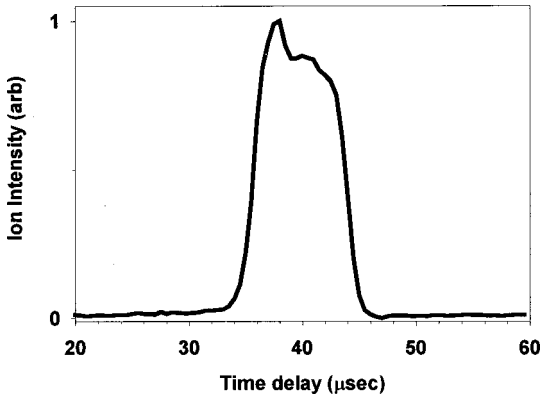

FIG. 2. He ion intensity as a function of the delay between the valve opening and ionizing pulses. The measured pulse width is 8 μs. Notice the ''flat top'' shape of the gas pulse indicating full opening of the valve. The arrival time of the gas pulse to the mass spectrometer (230 μs) allows us to calculate the He velocity at the operating temperature of 310 K (V=1780 $\pm$20 m/s).

Figure 3 is a spectrum of such a contour. We used a two-color two-photon threshold ionization scheme. Since the rotation constants of Aniline are well known in its ground and excited states,[14] the contour can be simulated accurately and can serve as a sensitive rotation thermometer.[5] Figure 4 shows the simulated contour for several temperatures. We used an asymmetric rotor program to calculate the rotation band contours[15] in the temperature range T_R=0.05–2.0 K. We used the high accuracy rotation constants for the 0–0 transition, obtained by Sinclair and Pratt.[14] The nuclear spin statistical weights for the K_a even/K_a odd levels, which are equal to 7/9 were taken into account.

By comparing the amplitudes and separation of the main peaks, we could determine the temperature to within $\pm$0.1 K. The rotational temperature of the Aniline molecule is 0.4 $\pm$0.1 K. Similar results were obtained for the Anthracene molecule cooled in this pulsed valve. Our high-pressure jet source enabled us to cool large aromatic molecules to much lower temperatures than those achieved in the past ($\sim$2 K). This increased cooling capability was obtained, together with a reduction in the required pump capacity due to the short opening time of the pulsed valve. The achieved low temperatures depopulated all vibrational levels to undetected levels.

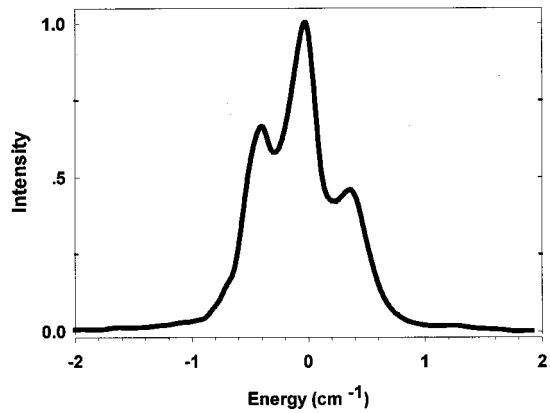

FIG. 3. Rotation contour of the 0–0 transition in Aniline. A comparison with simulation indicates a temperature of 0.4 K.

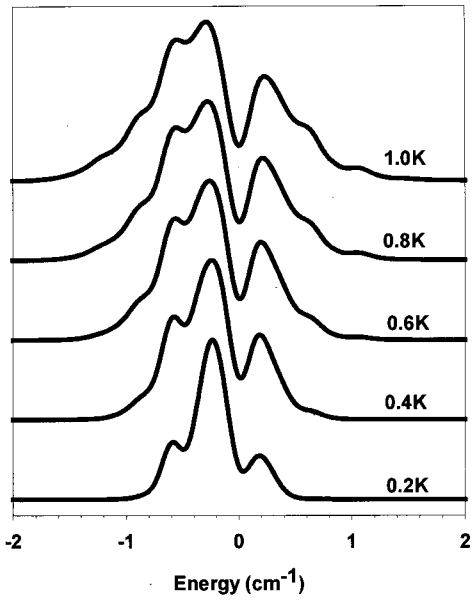

FIG. 4. Simulated rotation contour of Aniline at 0.2–1.0 K. Rotation constants from Ref. 14.

Figure 5 shows the mass-resolved spectra for Aniline–He_n ($n=0,1,2$). The width of the rotational contour does not increase significantly, even after clustering. Some low-frequency vibrations ($\sim 10\ cm^{-1}$) are evident in the clusters. The electronic origin of Aniline–He_n ($n=1,2$) clusters is red shifted relative to the electronic origin of the bare molecule ($\delta\nu \sim -1\ cm^{-1}$ for $n=1$ and $\delta\nu \sim -2\ cm^{-1}$ for $n=2$). The spectral shift enables us to use spectroscopic thermometry diagnostics of the bare molecule without interference from neighboring clusters.

IV. He CLUSTERS ON ANTHRACENE

Using two-photon, two-color, excitation, we obtained mass-resolved spectra of Anthracene–He clusters. One photon is scanned over the S_1 excitation region while the second photon is fixed at 2 cm^{-1} above the ionization threshold

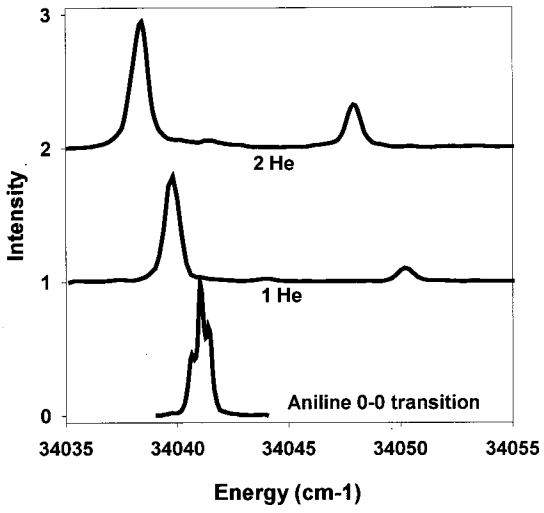

FIG. 5. Mass resolved spectra of Aniline–He clusters.

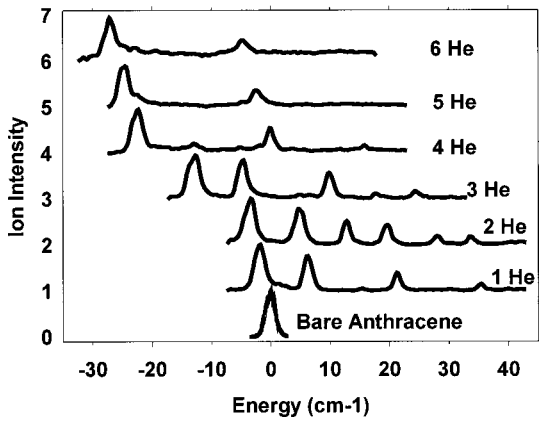

FIG. 6. Anthracene–He clusters excitation spectra near the 0–0 transition. The ionizing laser was kept at 2 cm^{-1} above the ionization threshold for each cluster.

energy for each cluster. The excitation spectra are shown in Fig. 6. The derived red shifts are in Fig. 7. The spectral shifts $\delta\nu_n$ of the electronic origin of Anthracene–He_n ($n=1-6$) clusters, which correspond to the lowest-energy excitation of each mass-selected cluster (Fig. 6), are to the red, manifesting the dominance of dispersive interactions for $\delta\nu$. The $n=1$ cluster reveals a low value of $\delta\nu_1=-1.6\ cm^{-1}$, which is attributed to the one-sided (1|0) structure. The $n=2$ cluster with $\delta\nu_2=-3.2\ cm^{-1}$ is assigned to the two-sided (1|1) cluster in view of the additivity relation $\delta\nu_2=2\,\delta\nu_1$. The large jump of $\delta\nu_3=-12.6\ cm^{-1}$ is attributed to the (2|1) structure for Anthracene–He_3. Accordingly, we can estimate the spectral shift of the one-sided (2|0) structure as $\delta\nu(2|0)=\delta\nu(2|1)-\delta\nu(0|1)=-11.0\ cm^{-1}$. The experimental spectral shift $\delta\nu_4=-21.9\ cm^{-1}$ for the $n=4$ cluster is assigned to the two-sided (2|2) structure, with the experimental value of $\delta\nu_4$ being in accord with the estimate $\delta\nu(2|2)=2\,\delta\nu(2|0)=-22.0\ cm^{-1}$. Finally, the $\delta\nu_5=-24.2\ cm^{-1}$ and $\delta\nu_6=-26.4\ cm^{-1}$ experimental values are assigned to the (3|2) for $n=5$ and (3|3) for $n=6$ structures, respectively, with the one-sided shift $\delta\nu(3|0)=-13.2\ cm^{-1}$. Only two-sided structures are exhibited for $n>1$. The corresponding one-sided structures are not observed, although the spectrum of **Anthracene–He_2** reveals a very weak feature at $\delta\nu=-11.8\ cm^{-1}$.

The Anthracene–He_n clusters reveal rather irregular spectral shifts, with an abrupt jump of $\delta\nu_n$ vs n at $n=3$ (Fig. 7), which is manifested by the surprisingly large ratio $\delta\nu(2|0)/\delta\nu(1|1)=3.47$. This behavior is in marked difference with the characteristics of Anthracene–Ar_n clusters, where the difference in the spectral shifts for the one-sided and the two-sided structures is small, i.e., $\delta\nu(2|0)/\delta\nu(1|1)=1.15$.[16,17] The marked three-fold difference between the one-sided and the two-sided structures may originate from quantum effects in the large-amplitude motion of He_2 on the microsurface of Anthracene, which will change the balance between the contribution of short-range blue shifts and the dispersive red shifts to the total spectral shift.

Finally, we note the extensive vibrational structure at higher energies above the electronic origin (Fig. 6). The vibrational frequencies of Anthracene–He(1|1) structure of (1)

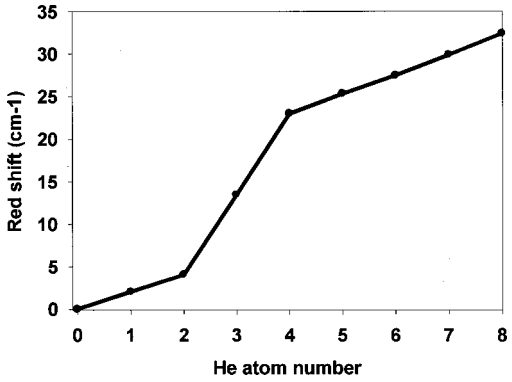

FIG. 7. Red shift of the electronic origin of He clusters on Anthracene.

8.1 cm^{-1}, (2) 22.9 cm^{-1}, (3) 37 cm^{-1}, and (4) 47 cm^{-1} are also manifested for the (1|1) structure of Anthracene–He_2, but with somewhat higher relative intensities at higher energies. The vibrational structure seems to disappear at higher cluster numbers. The elucidation of the manifestation of quantum effects and permutational symmetry will be of considerable interest.

[1] D. H. Levy, L. Wharton, and R. E. Smalley, in *Chemical and Biochemical Applications of Lasers*, edited by C. B. Moore (Academic, New York, 1977), Vol. 2, p. 1.
[2] S. M. Beck, D. L. Morris, M. G. Liverman, and R. E. Smalley, J. Chem. Phys. **70**, 1062 (1979).
[3] A. Amirav, U. Even, and J. Jortner, Chem. Phys. Lett. **51**, 31 (1980).
[4] D. Bahatt, O. Cheshnovsky, U. Even, N. Lavie, and Y. Magen, J. Phys. Chem. **91**, 2460–2462 (1987).
[5] A. Amirav, U. Even, J. Jortner, F. W. Birss, and D. A. Ramsay, Can. J. Phys. **61**, 278–287 (1983).
[6] N. Blackrishman, R. C. Foney, and Dalgano, Phys. Rev. Lett. **80**, 3224 (1998).
[7] A. Rioretti, D. Comparat, A. Crubellier, O. Dulieu, F. Manson-Seeuws, and P. Pillet, Phys. Rev. Lett. **80**, 4402 (1998).
[8] J. P. Toennies and A. F. Vilevos, Annu. Rev. Phys. Chem. **49**, 1 (1998).
[9] S. Goyal, D. L. Schutt, and G. Scoles, Phys. Rev. Lett. **69**, 933 (1992).
[10] R. Frochtenicht, J. P. Toennies, and A. Vilesov, Chem. Phys. Lett. **229**, 1 (1994).
[11] J. D. Weinstein, R. de Carvalho, T. Guillet, B. Freidrich, and J. M. Doyle, Nature (London) **395**, 148 (1998).
[12] PDE Solutions Inc., 38665 Fremont Blvd., Fremont, CA 94536.
[13] Mitsubishi Electric IGBT module CM600HA-12H.
[14] W. E. Sinclair and D. W. Pratt, J. Chem. Phys. **105**, 7942 (1996).
[15] L. Pierce, unpublished; version used given by K. K. Innes to J. E. Parkin and modified by the latter and by C. Cossart-Magos.
[16] E. Shalev, N. Ben-Horin, U. Even, and J. Jortner, J. Chem. Phys. **95**, 3147 (1991).
[17] D. Uridat, V. Brenner, I. Dimicoli, J. Le Calvé, P. Millie, M. Mons, and F. Piuzzi, Chem. Phys. **239**, 151 (1998).